Ain Shams Engineering Journal 10 (2019) 565–572

Contents lists available at ScienceDirect

Ain Shams Engineering Journal

journal homepage: www.sciencedirect.com

Engineering Physics and Mathematics

Analysis of unsteady viscous dissipative poiseuille fluid flow of two-step exothermic chemical reaction through a porous channel with convective cooling

S.O. Salawu [a,*], N.K. Oladejo [a], M.S. Dada [b]

[a] Department of Mathematics, Landmark University, Omu-Aran, Nigeria
[b] Department of Mathematics, University of Ilorin, Ilorin, Nigeria

ARTICLE INFO

Article history:
Received 14 April 2018
Revised 6 August 2018
Accepted 30 August 2018
Available online 21 February 2019

Keywords:
Dissipation
Poiseuille flow
Exothermic reaction
Convective cooling
Finite difference method

ABSTRACT

In this study, the viscous dissipation of heat transfer of poiseuille fluid flow of two-step exothermic chemical reaction through a porous channel is investigated under different chemical kinetics. The flow is pressure-driven past fixed plates with heat generation. The upper wall surface is exposed to heat exchange with the temperature of the ambient aligning with the Newton's law of cooling. The modeled coupled partial differential equations are non-dimensional and solved using stable and unconditional semi-implicit convergent finite difference method. The results are represented graphical and discussed accordingly for the velocity and temperature profiles showing the effect of some embodiment parameters entrenched in the system. From the results it was noticed that an increase in Frank-Kamenetskii parameters produces significant rises in the temperature distribution.

1. Introduction

The phenomena of spontaneous explosion as a result of internal heating in combustible materials, for example, coal, industrial waste fuel and wool waste can be demonstrated by thermal explosion theory Makinde [1]. In fact, the issue of assessing the critical regimes through separating the region of nonexplosive and explosive chemical reactions is the fundamental issue of the explosion theory [2,3]. The classical mathematical model of the problem was first presented by Frank-Kamenestkii.

Exothermic chemical reaction flows have industrial and engineering applications in polymer expulsion, atomic reactor plan, geophysics and energy storage systems. In respect of it applications, Hassan and Maritz [4] reported on the internal heat generated by reactive hydromagnetic fluid flow in a channel. The problem was solved using Adomian decomposition method, and the entropy generation in the system under different chemical kinetics was presented. Makinde and Anwar [5] investigated the inherent irreversibility in a reactive hydromagnetic flow. The assortment solutions to a reactive variable viscosity of Couette flow under Arrhenius chemical kinetics in the presence of exothermic reaction was presented by Gbadeyan and Hassan [6]. Inherent irreversibility of hydromagnetic third-grade reactive poiseuille flow of a variable viscosity in porous media with convective cooling was considered by Salawu and Fatunmbi [7]. The author, discussed the Sensitized, Arrhenius and Bimolecular chemical kinetics of a single step exothermic reaction. In the above studies, the attention was focused mainly on the steady state convection flow with a single step exothermic reaction of a reactive hydromagnetic fluid flow.

The numerical solution to unsteady hydromagnetic third-grade reactive liquid flow with convective cooling under the influence of variable viscosity was studied by Makinde and Chinyoka [8]. Natural convection of hydromagnetic reactive fluid in a vertical channel was investigated by Uwanta and Hamza [9]. The transient reactive hydromagnetic fluid flow was discussed without considering the two-step exothermic chemical reaction which is very essential in ignition processes as power generation, fire safety and prevention, pollution control, rocket and jet propulsion and materials processing industries.

* Corresponding author.
E-mail address: salawu.sulyman@lmu.edu.ng (S.O. Salawu).
Peer review under responsibility of Ain Shams University.

Production and hosting by Elsevier

https://doi.org/10.1016/j.asej.2018.08.006
2090-4479/

The important of two-step chemical reaction in combustion processes cannot be over emphasis due to it support in complete combustion of unburned ethanol Szabo [10]. This process helps in reducing the release into the environment the toxic car pollutant called carbon (II) oxide (CO). The thermal stability of a two-step exothermic chemical reaction in a slab was examined by Makinde et al. [11], considering the diffusion of reactant and assumed the variable pre-exponential factor for both transient and steady state. The authors also analyzed the critical regime, separating region of explosive and non-explosive ways of the two-step exothermic chemical reaction but ignored the effect of chemical kinetics on the flow. Recently, the problem of an unsteady reactive viscous combustible fluid flowing through a porous channel with radiation under different chemical kinetics in a two step exothermic chemical reaction was investigated by Kareem and Gbadeyan [12]. The authors coupled Laplace transform along with differential transform method to obtain solution to the problem under consideration.

The present study examine the unsteady reactive poiseuille fluid flow of two-step exothermic chemical reaction within two fixed walls in the presence of viscous dissipation and heat generation. The analysis is done under various chemical kinetics (i.e. Arrhenius, Sensitized and Bimolecular kinetics). Most of the existing studies relating to the study with convective cooling have been focused mainly on a single step exothermic chemical reaction under Arrhenius kinetics only. However, it is pertinent to note that to predict the fluid flow behaviour accurately in terms of velocity and temperature distributions, other chemical kinetics such as Sensitized and Bimolecular cannot be ignored. The problem formulation is developed in section two. The semi implicit finite difference scheme for the solution in space and time is presented in section three. The numerical results is graphically illustrated and quantitatively discussed in section four to show the effect of some parameters entrenched in the flow fluid system.

2. Problem formulation

Consider the flow of an unsteady incompressible reactive fluid with two-step exothermic chemical reaction taking place between two parallels fixed walls of width a. The flow is prompted by the action of axial pressure gradient applied in the flow direction. The wall lower surface is subjected to heat exchange with the temperature of the ambient. The $\bar{x}$-axis is assumed to be parallel to the plate while the $\bar{y}$-axis chosen to be perpendicular to it, as displayed in Fig. 1.

Following [13,11], ignoring the viscous reacting consumption fluid, the mechanism of two-step reaction, the momentum with temperature balance are demonstrated below;

Mechanisms of two-step reaction

$$C_2H_5OH + 2(O_2 + 3.76N_2) \rightarrow 2CO + 3H_2O + 7.52N_2$$

$$CO + 0.5(O_2 + 3.76N_2) \rightarrow CO_2 + 1.88N_2$$

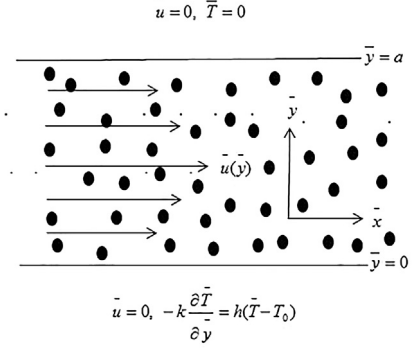

Fig. 1. Geometry of the flow.

The equations governing the flow

$$\frac{\partial \bar{u}}{\partial \bar{t}} = -\frac{1}{\rho}\frac{\partial \bar{p}}{\partial \bar{x}} + \frac{\mu}{\rho}\frac{\partial^2 \bar{u}}{\partial \bar{y}^2} - \frac{\mu \bar{u}}{\rho K_1} \tag{1}$$

$$\rho C_p \frac{\partial \overline{T}}{\partial \bar{t}} = k\frac{\partial^2 \overline{T}}{\partial \bar{y}^2} + \mu\left(\frac{\partial \bar{u}}{\partial \bar{y}}\right)^2 + \frac{\mu \bar{u}^2}{K_1} + Q_1 C_1 A_1 \left(\frac{K\overline{T}}{\upsilon l}\right)^m e^{\frac{E_1}{R\overline{T}}} + Q_2 C_2 A_2 \left(\frac{K\overline{T}}{\upsilon l}\right)^m e^{\frac{E_2}{R\overline{T}}} + Q_0(\overline{T} - T_w) \tag{2}$$

Subject to relevant boundary conditions

$$\begin{aligned} &\bar{u}(\bar{y},0) = 0, \quad \overline{T}(\bar{y},0) = T_0, \\ &\bar{u}(0,\bar{t}) = 0, \quad -k\frac{\partial \overline{T}}{\partial \bar{y}}(0,\bar{t}) = h(\overline{T}(0,\bar{t}) - T_w), \quad for\ \bar{t} > 0 \\ &\bar{u}(a,\bar{t}) = 0, \quad \overline{T}(a,\bar{t}) = T_w, \quad for\ \bar{t} > 0 \end{aligned} \tag{3}$$

where $\rho, C_p, k, \mu, \upsilon, l, R, Q_0, K, K_1$ and T_w are respectively fluid density, specific heat at constant pressure, thermal conductivity, fluid viscosity, vibration frequency, planck's number, universal gas constant, heat generation coefficient, Boltzmann's constant, Darcy porosity term and wall temperature respectively. Q_1, C_1, A_1 and E_1 are first step heat of reaction, reactant species concentration, reaction rate constant and activation energy while Q_2, C_2, A_2 and E_2 are the second step heat of reaction, reactant species concentration, reaction rate constant and activation energy respectively. The numerical exponents $m \in \{-2, 0, 0.5\}$ represents the chemical kinetics for Sensitized, Arrhenius and Bimolecular chemical kinetic respectively.

The following dimensionless parameters are used

$$\begin{aligned} &y = \frac{\bar{y}}{a}, \quad x = \frac{\bar{x}}{a}, \quad T = \frac{E_1(\overline{T} - T_w)}{RT_w^2}, \quad G = -\frac{\partial \bar{p}}{\partial \bar{x}}, \quad p = \frac{a\bar{p}}{\mu U}, \\ &\varphi = \frac{a^2}{K_1}, \quad Bi = \frac{ah}{k}, \quad u = \frac{\bar{u}}{U}, \\ &\lambda = \frac{Q_1 C_1 A_1 E_1 a^2}{kRT_w^2}\left(\frac{KT_w}{\upsilon l}\right)^m e^{\frac{1}{\epsilon}}, \quad Q = \frac{Q_0 RT_w^2}{Q_1 C_1 A_1 E_1}\left(\frac{\upsilon l}{KT_w}\right)^m e^{-\frac{1}{\epsilon}}, \quad \epsilon = \frac{RT_w}{E_1} \\ &\gamma = \frac{Q_2 C_2 A_2}{Q_1 C_1 A_1}, \quad Pr = \frac{\mu c_p}{k}, \quad t = \frac{\mu \bar{t}}{\rho a^2}, \quad r = \frac{E_2}{E_1}, \\ &Br = \frac{\mu U^2 E_1}{kRT_w^2}, \quad T_a = \frac{E_1(T_0 - T_w)}{RT_w^2}, \end{aligned} \tag{4}$$

Using the dimensionless parameters (4) on Eqs. (1)–(3), gives

$$\frac{\partial u}{\partial t} = G + \frac{\partial^2 u}{\partial y^2} - \varphi u \tag{5}$$

$$Pr\frac{\partial T}{\partial t} = \frac{\partial^2 T}{\partial y^2} + Br\left[\left(\frac{\partial u}{\partial y}\right)^2 + \varphi u^2\right] + \lambda\left[(1 + \epsilon T)^m\left(e^{\frac{T}{1+\epsilon T}} + \gamma e^{\frac{rT}{1+\epsilon T}}\right) + QT\right] \tag{6}$$

with the corresponding boundary conditions

$$\begin{aligned} &u(y,0) = 0, \quad T(y,0) = T_a, \\ &u(0,t) = 0, \quad \frac{\partial T}{\partial y}(0,t) = -BiT(0,t), \quad for\ t > 0 \\ &u(1,t) = 0, \quad T(1,t) = 0, \quad for\ t > 0 \end{aligned} \tag{7}$$

where $u, T, T_a, G, \varphi Br, \lambda, Bi, \gamma, Pr, \epsilon, r, t,$ and Q are respectively the dimensionless fluid velocity, fluid temperature, initial temperature parameter, pressure gradient, porosity parameter, Brinkman number, Frank-Kamenetskii parameter, Biot number, two-step exothermic reaction parameter, Prandtl number, activation energy parameter, activation energy ratio parameter, time and heat source parameter. The other non-dimensional quantities of engineering

interest are the skin friction (C_f) and the heat transfer rate at the wall (Nu) are given as

$$C_f = \frac{du}{dy}(1,t), \quad Nu = -\frac{dT}{dy}(1,t) \tag{8}$$

Hence, Eqs. (5)–(8) are numerically solved by semi-implicit finite difference scheme.

3. Method of solution

The computational algorithm embraced for the momentum and energy equations is semi-implicit finite difference scheme as in [15,14], the scheme takes implicit terms at the intermediary time level $(N+\xi)$ where $0 \leqslant \xi \leqslant 1$. In order to make immense time steps, ξ is taken to be 1. In fact, being totally implicit, the adopted numerical algorithm offered in this work is hypothesized to be appropriate for any estimation of time steps. The equations is discretarized on a cartesian linear mesh with homogenous grid on which the finite-differences are taken. Approximating the first and second spatial derivatives with central differences of second-order, the equations conforming to the last and first grid points are adapted to integrate the boundary conditions. The semi-implicit scheme for the momentum module takes the form:

$$\frac{\left(u^{(N+1)} - u^{(N)}\right)}{\Delta t} = u_{yy}^{(N+\xi)} + G - \varphi u^{(N+\xi)} \tag{9}$$

The equation for $u^{(N+1)}$ becomes:

$$\begin{aligned} &-w_1 u_{j-1}^{N+1} + (1 + 2w_1 + \varphi\Delta t)u_j^{N+1} - w_1 u_{j+1}^{N+1} \\ &\quad = u^{(N)} + \Delta t(1-\xi)u_{yy}^{(N)} + \Delta t G - \Delta t\varphi(1-\xi)u^{(N)} \end{aligned} \tag{10}$$

where $w_1 = \xi\Delta t/\Delta y^2$ while forward difference schemes are taken for all derivatives of time. The solution method for $u^{(N+1)}$ decreases to the tri-diagonal inversion matrices.

The semi-implicit scheme for the energy module resemble that of velocity equation. The unvaried second derivatives of the heat takes the form:

$$\begin{aligned} Pr\frac{T^{(N+1)} - T^{(N)}}{\Delta t} &= \frac{\partial^2 T^{(N+\xi)}}{\partial y^2} + Br\left[u_y^2 + \varphi u^2\right]^{(N)} \\ &\quad + \lambda\left[(1+\epsilon T)^m\left(e^{\frac{T}{1+\epsilon T}} + \gamma e^{\frac{rT}{1+\epsilon T}}\right) + QT\right]^{(N)} \end{aligned} \tag{11}$$

The equation for $T^{(N+1)}$ becomes:

$$\begin{aligned} &-w_2 T_{j-1}^{(N+1)} + (Pr + 2w_2)T_j^{(N+1)} - w_2 T_{j+1}^{(N+1)} \\ &\quad = T^{(N)} + \Delta t(1-\xi)T_{yy}^{(N)} + Br\Delta t\left[u_y^2 + \varphi u^2\right]^{(N)} \\ &\qquad + \lambda\Delta t\left[(1+\epsilon T)^m\left(e^{\frac{T}{1+\epsilon T}} + \gamma e^{\frac{rT}{1+\epsilon T}}\right) + QT\right]^{(N)} \end{aligned} \tag{12}$$

where $w_2 = \xi\Delta t/\Delta y^2$. The solution technique for $T^{(N+1)}$ also decreases to the tri-diagonal inversion matrices. The schemes (9) and (11) were tested for uniformity. When $\xi = 1$ enable us to take large time steps that is second order in space but first-order precise in time. As previously assumed, the scheme satisfies any time step values! The Maple code was used to carried out the numerical analysis.

4. Results and discussion

The initial temperature of the reactive fluid is taken to be the same as wall temperature, therefore parameter $T_a = 0$. The ranges of the adopted parameters values are based on existing theoretical results of [13,12,11].

Table 1 illustrates the effect of various fluid parameters under consideration on the thermal runaway for two-step exothermic chemical reaction. An increase in the parameters γ, Br, Q and r causes a reduction in the critical values (λ_c) of Frank-Kamenettski parameters because they leads to reduction in the thermal fluid layer that causes diffusion of heat away from the system while a revised behaviour is noticed with an increase in the parameter φ that leads to a rise in the critical values (λ_c) of Frank-Kamenettski parameter due to an enhancement in the heat content of the system. The reaction parameter λ need to be consciously checked and managed as large values can cause finite time temperature blow up of the solutions as presented in Table 1 because the terms related to λ are stronger source of heat.

It is interesting to note from Table 2 shows that explosion reaction in bimolecular takes place faster than the reactions in Senstitized and Arrhenius kinetics. The behaviour is as a result of bimolecular reaction with smaller value of the thermal criticality. An increase in the extent of thermal criticality is noticed with a diminish in the activation energies, therefore thermal stability is enhanced while thermal runaway is early discouraged.

The transient solutions on an even finer mesh ($\Delta t = 0.0001$ with $\Delta y = 0.01$) are displayed in Figs. 2 and 3. The figures portray a transient increase in both the fluid velocity and temperature until a steady state is reached. Figs. 4 and 5 represent the time of achieving steady state velocity and temperature profiles for different parameters values. That is, the time of obtaining no variation in the fluid momentum and energy distributions, the maximum velocity is obtained at $u_{max} = 0.1233$ and the maximum temperature is recorded at $T_{max} = 1214$.

Figs. 6 and 7 demonstrate the influence of variations in the pressure gradient G on fluid flow and temperature field. A rise in the pressure gradient causes an increase in the fluid velocity and heat content of the system i.e. the maximum velocity occurs as the pressure gradient increases which implies that the more the pressure is applied in the channel, the faster the fluid flow and the higher the temperature generated within the system due to an increase in the rate of fluid particles collision.

Fig. 8 depicts the response of the temperature to a rise in Prandtl number Pr. An increase in the parameter values of Pr causes decrease in the temperature distribution. This is because the boundary layer thickness and the strength of the source parameters in the temperature decreases that in turn diminish the total fluid temperature as evidently demonstrated in the figure.

Fig. 9 represents the influence of Brinkman number Br on the temperature distribution. It is noticed that a rise in the Brinkman number amplifies the energy field. The parameter Br is related to viscosity dissipation in the heat equation, and hence larger values of Br leads to a rise in the heat generated by the shear stress in the fluid thereby causing the fluid particles to moves freely and resulted to a rise in the fluid temperature.

Fig. 10 denotes the effect of varying in the values of two-step exothermic reaction parameter γ on the temperature profile. It is noticed that an increase in the parameter γ produces significant rises in the temperature distribution. This is because the thermal boundary layer gets thicker as the values of the parameter γ rises and thereby reduces the amount of heat that diffuse out of the system and in turn increases the temperature field. Therefore, a rise in the profile is an evidence that two-step exothermic chemical reaction support complete combustion of unburned ethanol in the engine which decreases the amount of carbon-monoxide that is releases into the environment.

Fig. 11 illustrates the effect of the term λ on the temperature field of the system. An increase in the Frank-Kamenetskii parameter λ enhances the temperature profile, this is opposite to the role play by the Prandtl number described above. Increasing the values of λ leads to a rise in the reaction rate and viscous heating source

Table 1
The effects of different parameters on the system blow up solutions.

r	Br	G	γ	φ	Q	m	ϵ	λ_c
1.0	1.0	1.0	1.0	0.1	0.5	0.5	0.5	0.14307817321101074
1.0	1.0	1.0	2.0	0.1	0.5	0.5	0.5	0.08463136436821836
1.0	2.0	1.0	1.0	0.1	0.5	0.5	0.5	0.13900376624897837
1.0	3.0	1.0	1.0	0.1	0.5	0.5	0.5	0.13519246785211794
1.0	1.0	1.0	1.0	0.2	0.5	0.5	0.5	0.14316085047224741
1.0	1.0	1.0	1.0	0.3	0.5	0.5	0.5	0.14324120784003946
1.0	1.0	1.0	1.0	0.1	1.0	0.5	0.5	0.13558848416143185
1.0	1.0	1.0	1.0	0.1	1.5	0.5	0.5	0.12885813171589758
2.0	1.0	1.0	1.0	0.1	0.5	0.5	0.5	0.06543286595758994
3.0	1.0	1.0	1.0	0.1	0.5	0.5	0.5	0.02643637641373641

Table 2
Comparison of computational results showing thermal criticality for different chemical kinetics $Br = G = \varphi = Q = G = Bi = 0,\ Pr = 1$.

				Makinde et al. [11]		Present results	
ϵ	r	m	γ	θ_{max}	λ_c	T_{max}	λ_c
0.1	0.1	0.5	0.0	1.420243875	0.932216072	1.420243779	0.932215990
0.1	0.1	0.5	0.1	1.476474346	0.897649656	1.476474410	0.897649705
0.1	0.1	0.5	0.2	1.529465440	0.866522770	1.529465402	0.866522738
0.1	0.1	0.0	0.1	1.585899049	0.953645221	1.585899112	0.953645281
0.1	0.1	−0.2	0.1	2.320778138	1.282091040	2.320778129	1.282099988
0.1	0.5	0.5	0.1	1.467926747	0.880606329	1.467926695	0.880606294
0.1	1.0	0.5	0.1	1.420243875	0.847469156	1.420243823	0.847469121
0.2	0.1	0.5	0.1	1.905274235	0.968086041	1.905274278	0.968086117
0.3	0.1	0.5	0.1	3.046841932	1.074421454	3.046841889	1.074421391

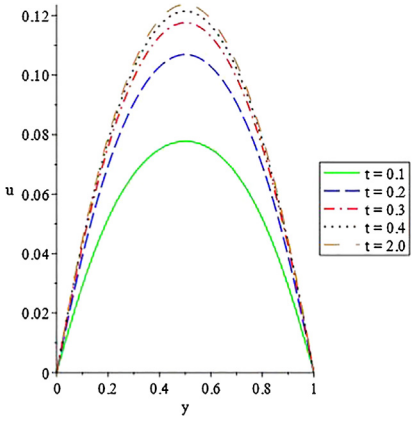

Fig. 2. Transient velocity profiles at $G = 1,\ P = 7.1,\ Br = 1,\ \gamma = 1,\ \lambda = 2,\ r = 1,\ m = 0.5,\ Bi = 0.5,\ \epsilon = 0.5,\ \varphi = 0.1$ and $Q = 0.5$.

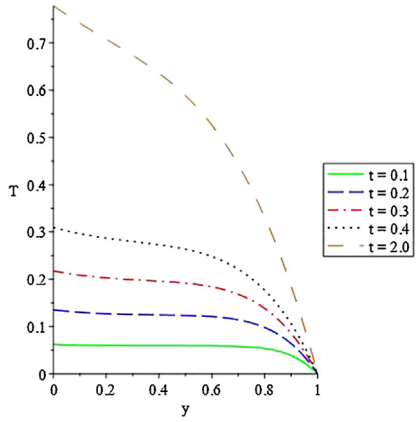

Fig. 3. Transient temperature profiles at $G = 1,\ P = 7.1,\ Br = 1,\ \gamma = 1,\ \lambda = 2,\ r = 1,\ m = 0.5,\ Bi = 0.5,\ \epsilon = 0.5,\ \varphi = 0.1$ and $Q = 0.5$.

terms, and hence meaningfully amplify the fluid temperature as shown in the Figure. The substantial rise in the temperature as a result of an increase in the term λ mean that the viscosity link to the velocity is strengthen and thereby gives rise to an increase in temperature field.

Figs. 12–14 respectively illustrate the influences of the Sensitized, Arrhenius and Bimolecular chemical kinetics on the temperature profile to a rise in the activation energy ϵ. It is observed that there is a significant reduction in the fluid temperature as the activation energy values increases for Sensitized, Arrhenius and Bimolecular chemical kinetics i.e. for the computational exponent $m = -2, m = 0$ and $m = 0.5$ respectively. Though, the effect of the activation energy are not the same under different chemical kinetics. More significant effect is noticed in the case of Bimolecular follow by Arrhenius then Sensitized chemical kinetics as a result of different effect on the reactive particles interaction rate. The chemical kinetic term represents the source terms in the energy equation.

Fig. 15 shows the impact of porosity term φ on the dimensionless velocity. It is noticed that the flow distribution reduces as the porosity parameter increases. This is due to the fact that the porosity medium gives rise to an additional opposition to the flow rate mechanism by influencing the free flow fluid to move at a retarding rate. While, Fig. 16 confirms the influence of the heat generation Q on the temperature profile. It is found that the temperature distribution rises speedily due to a rise in the parameter values Q. The figure specify that a rise in the parameter Q, build up the thermal boundary layer thickness which increases the amount of heat within the system and thereby reducing the quantity of energy transfer coefficient at the wall. Hence, an increase in the heat source reduces the fluid momentum viscosity and enhances the heat energy distribution within the reactive flow system.

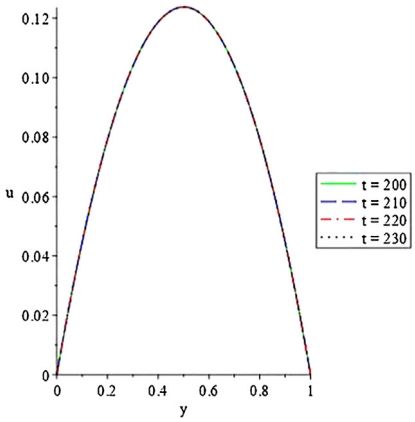

Fig. 4. Steady state velocity profiles at $G = 1$, $P = 7.1$, $Br = 1$, $\gamma = 1$, $\lambda = 2$, $r = 1$, $m = 0.5$, $Bi = 0.5$, $\epsilon = 0.5$, $\varphi = 0.1$ and $Q = 0.5$.

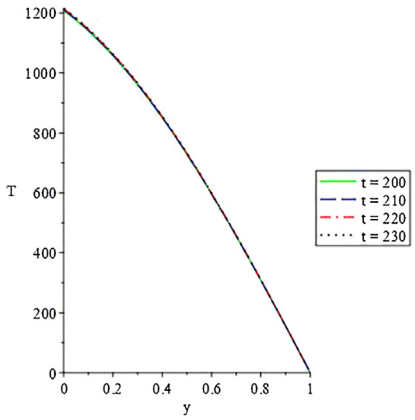

Fig. 5. Steady state temperature profiles at $G = 1$, $P = 7.1$, $Br = 1$, $\gamma = 1$, $\lambda = 2$, $r = 1$, $m = 0.5$, $Bi = 0.5$, $\epsilon = 0.5$, $\varphi = 0.1$ and $Q = 0.5$.

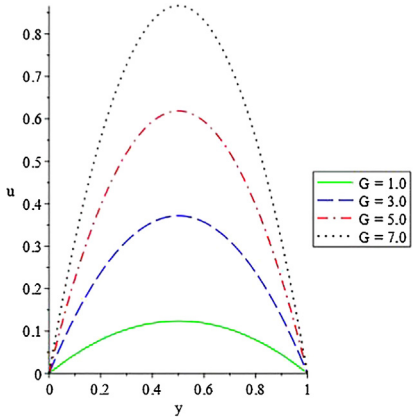

Fig. 6. Influences of (G) on velocity at $P = 7.1$, $Br = 1$, $\gamma = 1$, $\lambda = 2$, $r = 1$, $t = 5$, $m = 0.5$, $Bi = 0.5$, $\epsilon = 0.5$, $\varphi = 0.1$ and $Q = 0.5$.

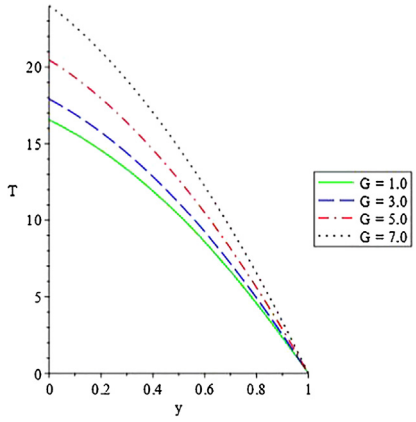

Fig. 7. Influences of (G) on temperature at $P = 7.1$, $Br = 1$, $\gamma = 1$, $\lambda = 2$, $r = 1$, $t = 5$, $m = 0.5$, $Bi = 0.5$, $\epsilon = 0.5$, $\varphi = 0.1$ and $Q = 0.5$.

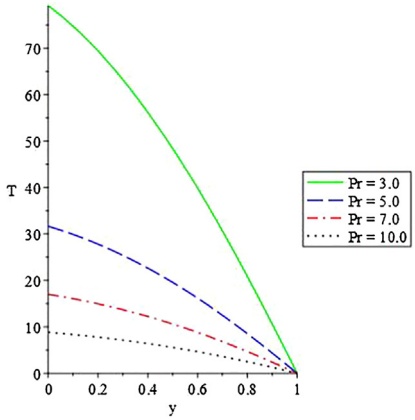

Fig. 8. Influences of (Pr) on temperature at $G = 1$, $Br = 1$, $\gamma = 1$, $\lambda = 2$, $r = 1$, $t = 5$, $m = 0.5$, $Bi = 0.5$, $\epsilon = 0.5$, $\varphi = 0.1$ and $Q = 0.5$.

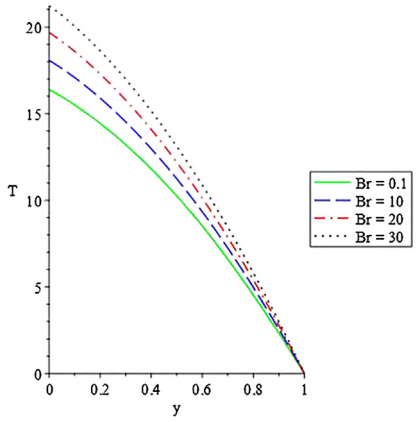

Fig. 9. Influences of (Br) on temperature at $G = 1$, $P = 7.1$, $\gamma = 1$, $\lambda = 2$, $r = 1$, $t = 5$, $m = 0.5$, $Bi = 0.5$, $\epsilon = 0.5$, $\varphi = 0.1$ and $Q = 0.5$.

Figs. 17 and 18 show the variations of the wall shear stress to an increase in the pressure gradient G and porosity term φ. An initial increase in the shear stress close to the wall is seen Fig. 17 as the parameter values G increases which later decreases as it moves away from the channel wall at $\gamma \geqslant 0.5$ while converse behaviour is observed as the parameter values φ is increasing for Fig. 18. An early decrease is noticed close to the wall but later rises far away from the wall towards the free flow under the influence of second step exothermic chemical reaction parameter.

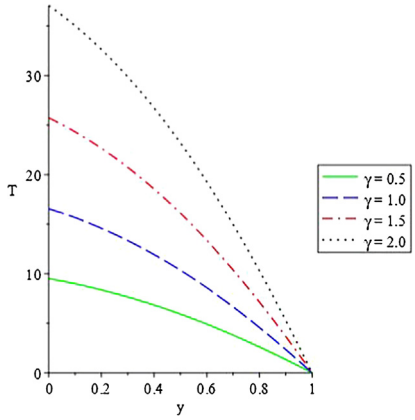

Fig. 10. Influences of (γ) on temperature at $G = 1,\ P = 7.1,\ Br = 1,\ \lambda = 2,\ r = 1,\ t = 5,\ m = 0.5,\ Bi = 0.5,\ \epsilon = 0.5,\ \varphi = 0.1$ and $Q = 0.5$.

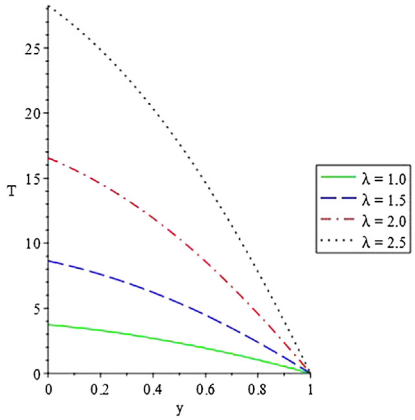

Fig. 11. Influences of (λ) on temperature at $G = 1,\ P = 7.1,\ Br = 1,\ \gamma = 1,\ r = 1,\ t = 5,\ m = 0.5,\ Bi = 0.5,\ \epsilon = 0.5,\ \varphi = 0.1$ and $Q = 0.5$.

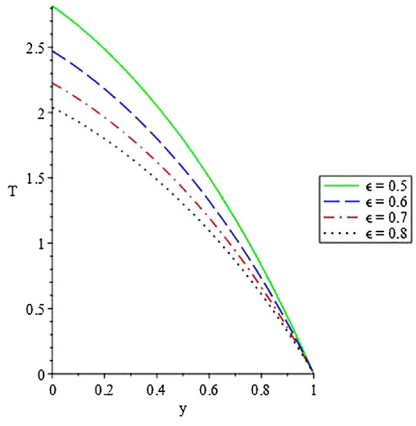

Fig. 12. Influences of (ϵ) on temperature when $m = -2$ at $G = 1,\ P = 7.1,\ Br = 1,\ \gamma = 1,\ \lambda = 2,\ r = 1,\ t = 5,\ Bi = 0.5,\ \varphi = 0.1$ and $Q = 0.5$.

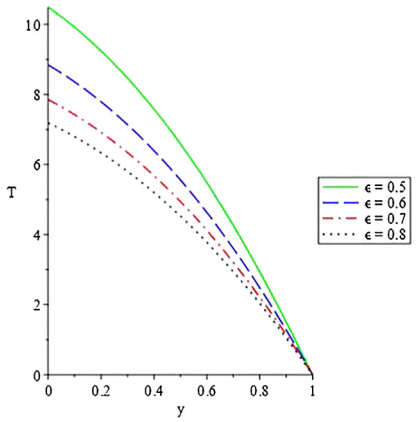

Fig. 13. Influences of (ϵ) on temperature when $m = 0$ at $G = 1,\ P = 7.1,\ Br = 1,\ \gamma = 1,\ \lambda = 2,\ r = 1,\ t = 5,\ Bi = 0.5,\ \varphi = 0.1$ and $Q = 0.5$.

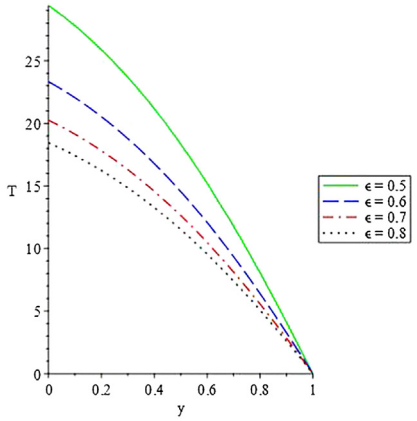

Fig. 14. Influences of (ϵ) on temperature when $m = 0.5$ at $G = 1,\ P = 7.1,\ Br = 1,\ \gamma = 1,\ \lambda = 2,\ r = 1,\ t = 5,\ Bi = 0.5,\ \varphi = 0.1$ and $Q = 0.5$.

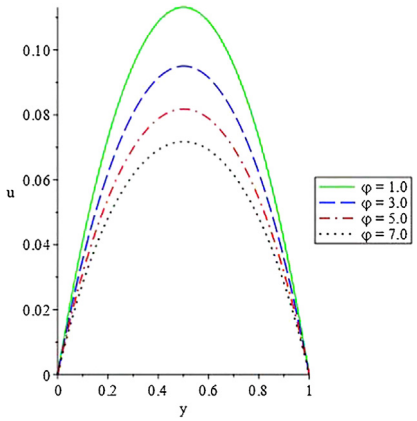

Fig. 15. Influences of (φ) on velocity at $G = 1,\ P = 7.1,\ Br = 1,\ \gamma = 1,\ \lambda = 2,\ r = 1,\ t = 5,\ m = 0.5,\ Bi = 0.5,\ \epsilon = 0.5$ and $Q = 0.5$.

Figs. 19 and 20 depict the variation of wall heat transfer rate to an increase in the Brinkman number *Br* and heat source *Q* parameters. There is respectively increase in the thermal gradient heat transfer rate at the wall as the parameter values *Br* and *Q* increasing. Both parameters enhances energy transfer coefficient at the wall by causing the reactive fluid particles to collide faster which leads to generation and distribution of more heat along the channel surface.

5. Conclusion

The reactive fluid flow of a two-step exothermic chemical reaction through fixed channel with upper wall convective cooling

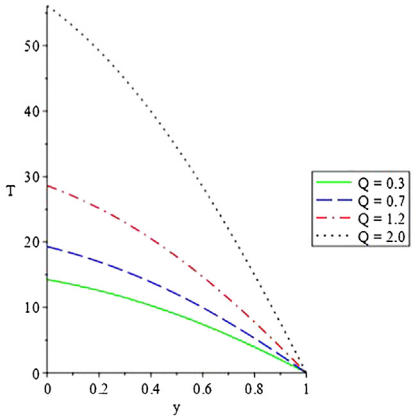

Fig. 16. Influences of (Q) on temperature at $G = 1,\ P = 7.1,\ Br = 1,\ \gamma = 1,\ \lambda = 2,\ r = 1,\ t = 5,\ m = 0.5,\ Bi = 0.5,\ \epsilon = 0.5$ and $\varphi = 0.1$.

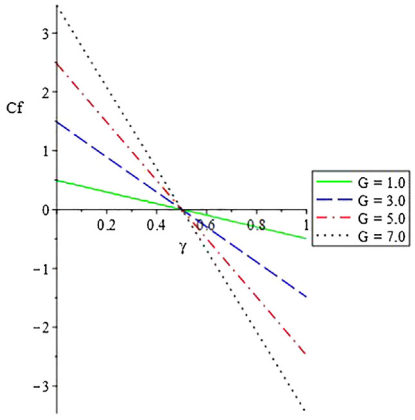

Fig. 17. Variation of wall shear stress with (γ) and (G) at $P = 7.1,\ Br = 1,\ \lambda = 2,\ r = 1,\ t = 5,\ m = 0.5,\ Bi = 0.5,\ \epsilon = 0.5,\ \varphi = 0.1$ and $Q = 0.5$.

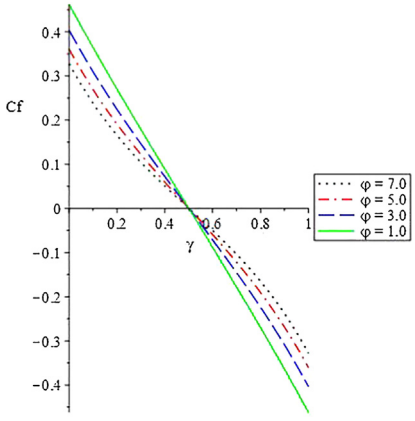

Fig. 18. Variation of wall shear stress with (γ) and (φ) at $G = 1,\ P = 7.1,\ Br = 1,\ \lambda = 2,\ r = 1,\ t = 5,\ m = 0.5,\ Bi = 0.5,\ \epsilon = 0.5$ and $Q = 0.5$.

have been investigated. The nonlinear dimensionless equations governing the flow was solved using stable and unconditional semi-implicit convergent finite difference method. It was observed that the temperature within the system reduces as activation energy increases under different chemical kinetic also the internal heat generation has great influence on the properties of fluid flow.

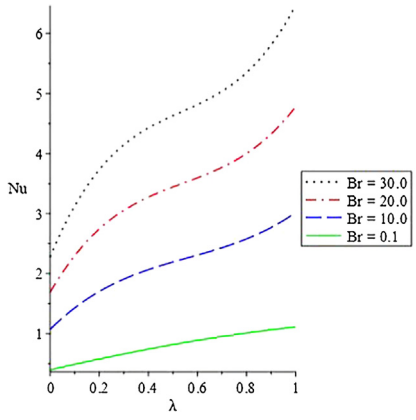

Fig. 19. Variation of wall heat transfer rate with (λ) and (Br) at $G = 1,\ P = 7.1,\ \gamma = 1,\ r = 1,\ t = 5,\ m = 0.5,\ Bi = 0.5,\ \epsilon = 0.5,\ \varphi = 0.1$ and $Q = 0.5$.

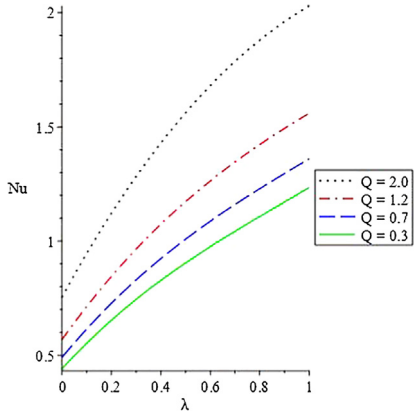

Fig. 20. Variation of wall heat transfer rate with (λ) and (Q) at $G = 1,\ P = 7.1,\ Br = 1,\ \gamma = 1,\ r = 1,\ t = 5,\ m = 0.5,\ Bi = 0.5,\ \epsilon = 0.5$ and $\varphi = 0.1$.

Moreover, two-step exothermic chemical reaction parameter γ produces a significant rises in the temperature profiles that support complete combustion of unburned ethanol within the chemical reactive flow system. A transient increase in the temperature is observed with an increase in the Frank-Kamenetskii at low values, whereas higher values of this parameter result to blow up of effect. The finite possible time blow up of solutions means also that the reaction strength needs to be carefully managed and controlled.

References

[1] Makinde OD. Exothermic explosions in a slab: a case study of series summation technique. Int Heat Mass Transfer 2004;31(8):1227–31.
[2] Frank-Kamenettskii DA. Diffusion and heat transfer in chemical kinetics. New York: Plenum Press; 1969.
[3] Balakrishnan E, Swift A, Wake GC. Critical values for some non-class A geometries in thermal ignition theory. Math Comput Modell 1996;24:1–10.
[4] Hassan AR, Maritz R. The analysis of a reactive hydromagnetic internal heat generating poiseuille fluid flow through a channel. Springer Plus 2016;5:1332.
[5] Makinde OD, Anwar Beg O. On inherent irreversibility in a reactive hydromagnetic channel flow. J Therm Sci 2010;19(1):72–9.
[6] Gbadeyan JA, Hassan AR. Multiplicity of solutions for a reactive variable viscous Couette flow under Arrhenius Kinetic. Math Theory Modell 2012;2(9):39–49.
[7] Salawu SO, Fatunmbi EO. Inherent irreversibility of hydromagnetic third-grade reactive poiseuille flow of a variable viscosity in porous media with convective cooling. J Serb Soc Comput Mech 2017;11(1):46–58.
[8] Makinde OD, Chinyoka T. Numerical study of unsteady hydromagnetic generalized Couette flow of a reactive third grade fluid with asymmetric convective cooling. Comput Math Appl 2011;61:1167–79.

[9] Uwanta IJ, Hamza MM. Unsteady natural convection flow of reactive hydromagnetic fluid in a moving vertical channel. Int J Energy Technol 2014;6(9):1–7.
[10] Szabo ZG. Advances in kinetics of homogeneous gas reactions. Great Britain: Methusen and Co Ltd; 1964.
[11] Makinde OD, Olanrewaju PO, Titiloye EO, Ogunsola AW. On thermal stability of a two-step exothermic chemical reaction in a slab. J Math Sci 2013:1–15.
[12] Kareem RA, Gbadeyan JA. Unsteady radiative hydromagnetic internal heat generation fluid flow through a porous channel of a two-step exothermic chemical reaction. J Nig Ass Math Phys 2016;34:111–24.
[13] Chinyoka T, Makinde OD. Numerical investigation of entropy generation in unsteady MHD generalized Couette flow with variable electrical conductivity. Scientif World J 2013:1–11.
[14] Chinyoka T. Computational dynamics of a thermally decomposable viscoelastic lubricant under shear. Trans ASME, J Fluids Eng 2008;130 (12):201–8.
[15] Chinyoka T, Renardy YY, Renardy M, Khismatullin DB. Two-dimensional study of drop deformation under simple shear for Oldroyd-B liquids. J Non-Newton Fluid Mech 2005;31:45–56.